Journal of Petroleum Engineering & Technology
Volume 1, Issue 1-3 Compilation 2011

STM JOURNALS

Formation of Reaction Bubbles in FCC Riser Reactor

*A. Sai Krishna Reddy and Vineet Kumar**
Department of Chemical Engineering, Indian Institute of Technology Roorkee, Roorkee, India

ABSTRACT

For modeling FCC unit, art of defining undefined hydrocarbon misxtures in conjunction with application of two different specialized fields of Chemical Engineering–Chemical Reaction Engineering (CRE) and Computational Fluid Dynamics (CFD) are required. CRE needs elaboarte and appropriate definition of undefined mixture and their chemical kinetics, whereas CFD needs solution of more regorous differential equations to define fluctuating and turbulent flow. Most of the reported works in available literature seems to be strong in only one field. To bridge this gap, in the present work a commercially availble CFD simulation package with k–epsilon turbulence model is used to solve a more regorous and realistic definition of cracking kinetics. The results obtained revealed that in the emulsion phase of fluidized bed, a new "reaction bubble" phase exist. Bubbles of non uniform reaction zones are formed inside emulsion phase where mass distribution of catalyst is fairly uniform.

Keywords: *Fluid Catalytic Cracking (FCC), Riser Modeling, Riser Hydrodynamics, Computational Fluid*

Author for Correspondence E-mail: vk.chemical@gmail.com

INTRODUCTION

Fluid catalytic cracking (FCC) unit of a refinery converts gas oil (heavy petroleum fractions having boiling range 370–600°C) to more valuable lighter products such as LPG and gasoline by catalytic cracking. The feedstock (gas oil) is normally preheated to about 370°C and then injected at the bottom of a vertical tubular reactor in atomized state along with hot regenerated catalyst at about 650 to 730°C. The atomized feed vaporizes almost instantaneously and sufficient upward thrust is generates that lifts catalyst up along the riser height in fluidized state.

During catalyst flight from bottom to top of the riser, further molar expansion occurs due to catalytic cracking of hydrocarbon vapor in contact with hot catalyst. Heat of reaction required for the endothermic cracking of hydrocarbons leads to cooling of catalyst. Coke is also produced during cracking of hydrocarbon. This coke gets deposited on catalyst surface leading to deactivation of catalyst. At the top of the riser, spent catalyst at about 400°C is separated from hydrocarbon vapor by steam stripping.

After steam stripping, the deactivated catalyst is fed to the regenerator where coke on catalyst surface is burnt in presence of air to regenerate and heat the catalyst up to 650 to 730 °C. Hot, regenerated catalyst is transported back to the riser. Hence, continuous catalyst circulation between the riser and the regenerator is maintained. A more elaborate discussion on design, working, and economics of FCC unit is presented by

Gray and Handwerk [1].

Because of the importance of FCC unit in refining, considerable efforts have been made for the modeling of this unit. In last five decades, the mathematical models of FCC unit have matured in many ways but unfortunately not a single model has come to the satisfaction of all refiners. Most models rely upon evaluation of rate constants using plant or experimental data that restrict adaptability of the model in some other plant. Complexity of the FCC process is mainly because of unknown reacting species and partly due to complex hydrodynamics of the riser reactor. Recently, a new generic approach of FCC modeling [2] has come up that considered cracking kinetics in greater detail but in this model hydrodynamic calculations were based on a simplified approach assuming one-dimensional two-phase plug-flow. In the present work, the same kinetic model of Gupta et al. [2] is applied on commercial software [3] to accommodate more rigorous hydrodynamics.

This combination of rigorous hydrodynamics and realistic kinetics led to visualization of an interesting phenomenon of 'bubbling reaction'. It was observed that although the gas and solids volume fraction are almost uniformly distributed inside the riser, but the rate of reaction is not uniform leading to some intense reaction and some non–reacting zones that moves like a bubble in fluidized bed. Mechanism of formation of such invisible reaction bubbles are discussed elsewhere [4]. This paper concludes that formation of such reaction bubbles leads to requirement of greater riser height as compared to model predictions.

MATHEMATICAL MODEL

Mathematical Models of FCC consists of two parts, one for the consideration of hydrodynamics of fluid-particle systems (hydrodynamic model), and second for the modeling of cracking reactions of unknown hydrocarbon mixtures (kinetic model). Beginning of the modern kinetic modeling of FCC unit may be considered as the work of Weekman and Nace [5–6] in which they modeled cracking of gas oil assuming second order conversion reactions of three lumped species, viz., gas oil (feed), gasoline, and rest of the materials (as Coke+Gas). The concept was further nurtured by many authors and several lumps have been evolved, e.g., 4-lump model, [7] 5–lump model, [8] and 10–lump model, [9] are some of the popular models among the theoretical investigators. However, Weekman's concept of conversion from one lump to other by various non-first–order reaction steps remained common in all these models. Recently, we have pointed out that a cracking reaction should be of first order and after cracking of one molecule at least two other molecules must form. [2] With these in view, we proposed a pseudo–component based kinetic model in which fifty components

(seven light–end and 43 hypothetical or pseudo-components) were considered that lead to about ten thousand possible first order reactions. Solutions of this model assuming one-dimensional plug flow are presented elsewhere. [2, 10, 11] In the present case, the same kinetic model is used with a more rigorous 3–dimensional k–ε model for two phase turbulent flow. For the sake of completeness, brief discussions about these models are given below.

Kinetic Model

The kinetic model assumes that the feed is composed of a few manageable numbers of hypothetical lumps (pseudo–components) of close boiling species and products formed are some light–end compounds and some other lighter pseudo–components. Generation and characterization of these pseudo-components were made by using method proposed by Miquel and Castells. [12, 13] which generates pseudo–components on the basis of boiling point and not on the basis of carbon number. It was further assumed that when one mole of a component (whether light–end– or pseudo-component) cracks it gives one mole each of two other lighter components. This kinetic model can be expressed as following pseudo reaction mechanism,

$$C_i \xrightarrow{k_{i,m,n}} C_m + C_n + \alpha_{i,m,n} \quad (1)$$

where i, m, and n are pseudo-components' numbers, $\alpha_{i,m,n}$ is the amount of coke formed (expressed in kg) when one kmol of i^{th} pseudo-component cracks and one kmole each of m^{th} and n^{th} components are formed. $\alpha_{i,m,n}$ can be calculated by the equation

$$\alpha_{i,m,n} = MW_i - (MW_m + MW_n) \quad (2)$$

In contrast to the original fifty components based kinetic model, in the present case only 14 components (seven light–end, C_1 to C_7 and seven pseudo–components, C_8 to C_{14}) were considered. The feed was assumed to be made of two pseudo-components (C_{13} and C_{14}). This reduction in number of components reduced the number of parallel reactions to 266 as compared to about ten thousand of the original model. Reduction in number of reactions was necessary as in the software used for present study, separate forms have to be filled to incorporate each individual reaction step. Detailed discussion about other parameters required for complete modeling of reaction is discussed in the 'Simulation' section.

To explain the reaction mechanism adopted in the present work, a schematic diagram showing 14 components and their possible cracking products is given in Figure 1. Same components are shown as numbered blocks in three columns (Reactant, Product 1, and Product 2). Numbering of components is done in increasing order of molecular weight/boiling point. According to this model, when any i^{th} component (say, the 13th pseudo-component shown in Figure 1) cracks, it gives

a pair of pseudo-components C_m, (C_{12}, in Fig.1) and C_n (any one out of C_1 to C_8) along with some amount of coke as cracking byproduct. Formation of any product heavier than C_8 is not possible when one molecule of C_{12} is formed upon cracking of C_{13} since sum of the molecular

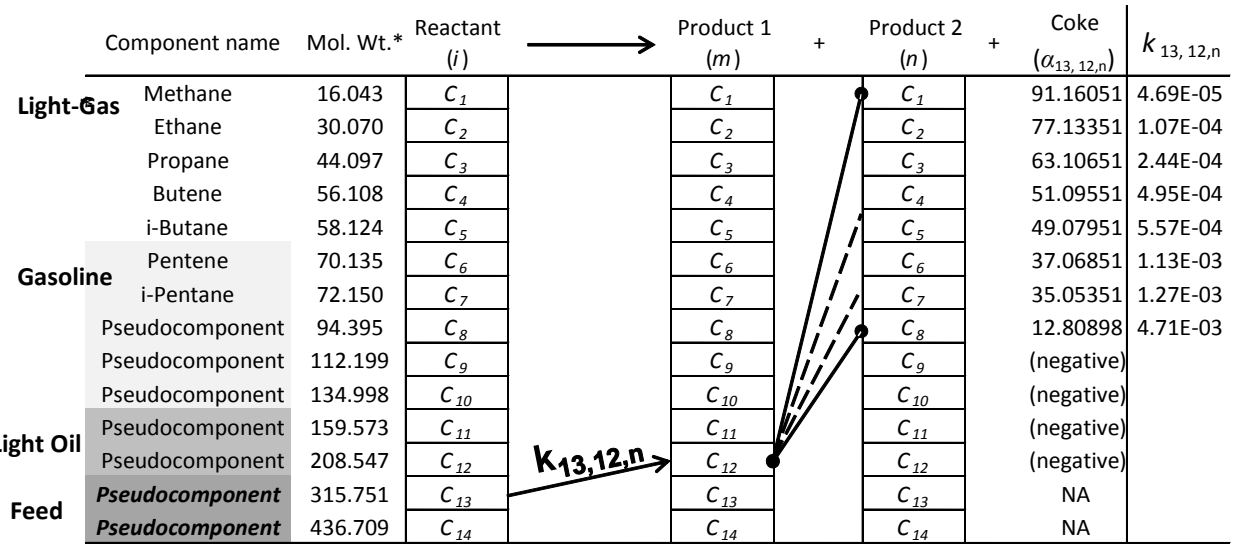

From Edmister and Lee [14] $Mol.Wt. = 204.38.e^{(0.00218T_b)}.e^{(-3.07.Sg)}.T_b^{0.118}.Sg^{1.88}$, where T_b and Sg are normal boiling point and specific gravity, respectively.

Fig. 1 A Schematic Diagram with Rate Constant of the Reaction Mechanism.

weights of products cannot be more than the molecular weight of reactant (law of mass action). Thus cracking of C_{13} giving C_{12} can take place through eight parallel reactions. Similarly, cracking of C_{13} giving C_{11} can take place through ten parallel reactions and cracking of C_8 giving C_6 is possible through only two parallel reactions in which C_6 and C_1, or C_6 and C_2 are formed. Here it is worth mentioning that although C_8 is not present in the feed, but its cracking is unavoidable when it comes in contact with hot catalyst after it is formed during cracking of a heavier component like C_{13} and C_{14}. Rate of reaction of these parallel reactions are, however, different in all cases.

Following equation to predict reaction rate for the cracking of any i^{th} pseudo-component was adopted from Gupta et al [2] ,

$$k_{i,m,n} = \left[0.01 \frac{e^{-\alpha_{i,m,n}/17} - e^{-MW_i}}{1 - e^{-MW_i}} \right] e^{-\frac{\left[1540 MW_i^{0.43}\right]}{RT}} \quad (3)$$

In the above equation, parameters given within square brackets are, respectively, pre–exponential factor and activation energy

parameters of Arrhenius equation. Also, it is evident from the Fig. 1 that when one kmole of C_{13} cracks to form one kmole each of C_{12} and C_2, 77.13351 kg of coke will form and the corresponding rate constant ($k_{13,\ 12,\ 2}$) is 1.07×10^{-4} (s^{-1}).

Hydrodynamics

Basis of any CFD problem modeling is the solution of Navier-Stokes equations, which is define for any single-phase continuous fluid flow. Governing (conservation) equations in general form is

$$\frac{\partial}{\partial t}\iiint_V \rho\phi dV + \iint_S \rho\phi\vec{u}\cdot d\vec{A} = \iint_S \Gamma_\phi \vec{\nabla}\phi \cdot d\vec{A} + \iiint_V S_\phi dV \quad (4)$$

where A is the surface area, V is the volume, and S is the source term.

The above equation represents conservation of mass, momentum, and energy when ϕ is 1, velocity component (u, v, w), and E, respectively.

Common technique for modeling gas-solid riser unit is Eulerian–Lagrangian approach, in which gas is treated as continuous phase and solids as discrete phase. In this approach transport parameters are estimated by using empirically determined correlations and coefficients. Some of the correlations and equations used in the simulation software for the estimation of transport parameters such as gas–particle interactions and particle–particle collisions terms are briefly discussed below.

Inter-phase exchange coefficients, β, is defined as

$$\beta = \frac{3}{4} C_D \frac{\varepsilon_s \varepsilon_g}{\nu^2_{r,s}} \frac{\rho_g}{d_s} \left(\frac{\mathrm{Re}_s}{\nu_{r,s}} \right) \left| U_s - U_g \right| \quad (5)$$

where subscript s and g refers to solid and gas phase, $v_{r,s}$ is the terminal velocity and ε, ρ, d and U are void fraction, density, particle diameter, and velocity, respectively. The drag coefficient, C_D is given by:

$$C_D = \left(0.63 + \frac{4.8}{\sqrt{\mathrm{Re}_s / \nu_{r,s}}} \right)^2 \quad (6)$$

$$\text{where} \quad \mathrm{Re}_s = \frac{\rho_g d_s \left| U_s - U_g \right|}{\mu_g} \quad (7)$$

The terminal velocity, $v_{r,s}$ for the solid phase is given by:

$$\nu_{r,s} = 0.5 \sqrt{\left[\begin{array}{c} (0.06\,\mathrm{Re}_S)^2 + 0.12\,\mathrm{Re}_S (2B - A) \\ + A^2 + 0.5A - 0.03\,\mathrm{Re}_S \end{array} \right]} \quad (8)$$

In above equation, $A = \varepsilon_g^{4.14}$ and $B = 0.8\varepsilon_g^{1.28}$ when $\varepsilon_g \leq 0.85$, and $B = 0.8\varepsilon_g^{2.65}$ when $\varepsilon_g > 0.85$

Another major issue in CFD is the fluctuating velocity fields. Velocity fluctuations are characteristics of the turbulent flows which is represented by the sum of mean velocity ($\bar{u}_i$) and a fluctuating velocity (u_i') as

$$u_i = \overline{u_i} + u_i' \qquad (9)$$

In order to predict turbulence (fluctuating velocity, u_i') several models are available. Unfortunately no single turbulence model is universally accepted as being superior for all classes of problems. The choice of turbulence model depends on considerations such as the physics encompassed in the flow, the established practice for a specific class of problem, the level of accuracy required, the available computational resources, and the amount of time available for the simulation. [3] However, two methods, RANS (Reynolds-averaged Navier–Stokes), and LES (Large-eddy Simulation) are widely used in turbulent flow simulation. Two methods have been developed to transform the Navier–Stokes equations so that the small–scale turbulent fluctuation is not simulated directly. Both methods introduce additional terms in the governing equations in order to incorporate turbulent kinetic energy (k) and its dissipation rate (ε). This approach is commonly known as k-ε model.

The velocities and other variables are based on Reynolds-averaged values and the effect of turbulence is represented by the Reynolds stresses which is evaluated by using turbulent viscosity defined as

$$\mu_t = \rho C_\mu \frac{k^2}{\varepsilon} \qquad (10)$$

The turbulent kinetic energy and its dissipation rate are obtained from the following transport equations:

$$\frac{\partial(\rho k)}{\partial t} + \frac{\partial(\rho u_i k)}{\partial x_i} = \frac{\partial}{\partial x_j}\left[\left(\mu + \frac{\mu_t}{\sigma_k}\right)\frac{\partial k}{\partial x_j}\right] + G_k + G_b - \rho\varepsilon \qquad (11)$$

and

$$\frac{\partial(\rho\varepsilon)}{\partial t} + \frac{\partial(\rho u_i \varepsilon)}{\partial x_i} = \frac{\partial}{\partial x_j}\left[\left(\mu + \frac{\mu_t}{\sigma_k}\right)\frac{\partial \varepsilon}{\partial x_j}\right] + C_{1\varepsilon}\frac{\varepsilon}{k}\{G_k + (1 - C_{3\varepsilon})G_b\} - C_{2\varepsilon}\rho\frac{\varepsilon^2}{k}. \qquad (12)$$

In these equations, G_k is the generation of turbulent kinetic energy due to the turbulent stress, and is defined by:

$$G_k = \left(-\overline{\rho u_i' u_j'}\right)\frac{\partial u_j}{\partial x_i} \qquad (13)$$

and the generation of turbulent kinetic energy due to buoyancy (G_b) is given by

$$G_b = \beta_t g_i \frac{\mu_t}{\mathrm{Pr}_t}\frac{\partial T}{\partial x_i} \qquad (14)$$

Here, Pr_t is the turbulent Prandtl number, g_i is the component of acceleration due to gravity in i^{th} direction and β_t is the thermal expansion coefficient given by

$$\beta_t = \frac{1}{\rho}\left(\frac{\partial \rho}{\partial t}\right)_P \qquad (15)$$

The software manual [3] claims that the default values of the constants appearing in equations (10) through (15), are $C_{1\varepsilon}$=1.44, $C_{2\varepsilon}$=1.92, C_{μ}=0.09, σ_k=1.0, σ_ε=1.3, and Pr_t=0.85 which work well for a wide range of wall-bounded and free shear flows. In the present work only these default values of coefficients were used.

Simulation

Simulation of any problem using FLUENT® is done in three steps, (i) definition of boundary conditions including geometry, type of boundary conditions, etc., using a preprocessor, (ii) definition of operating parameters including components, reaction rate constants, and (iii) execution to get results. In first step, suitable mesh was generated for solving the problem in a preprocessor. Since riser reactor is a cylinder of diameter 0.8 m and height 33 m, total 143226 hexahedral volume elements of 0.05 interval size were generated. Characteristics of each element is determined by its skewness that lies between 0 and 1, where 0 represents an ideal element, i.e., perfectly aligned and well shaped elements. Analysis of the quality of mesh generated revealed that all 143226 elements were active and skewness of 64.81% elements was less than 0.1; for 84.25% elements it was less than 0.2, and almost all (99.38%) elements had skewness less than 0.4.

Table I: Physical Properties of Pure and Pseudo-components.

Component		*Mw*[14]	*Boiling point*	*Gas** Density*	*CP*	*Thermal conductivity*	*Viscosity*	*Sat. Vap. Pressure*	*Droplet surface tension*	*ΔH*[16] *vaporization*	*Entropy*[17]
ID	Name	(kg/kmol)	(K)	(Kg/m^3)	(J/Kg-K)	(W/m-K)	(Kg/m-s)	(Pascal)	(n/m)	(J/kgmol-K)	(J/kgmol-K)
C_1	Methane	16.043	111.7	1.14310	2817.6	2.85E-05	6.64E-05	469734.8	0.00552	-7988303	75803.58
C_2	Ethane	30.070	184.5	2.14255	3205.8	2.86E-05	7.95E-05	361873.3	0.00865	-1.4E+07	79979.54
C_3	Propane	44.097	231.1	3.14199	3225.1	2.86E-05	8.58E-05	300716.5	0.01025	-1.8E+07	81851.50
C_4	i-Butene	56.108	266.9	3.99781	3199.0	2.86E-05	9.03E-05	263180.2	0.01137	-2.2E+07	83049.27
C_5	n-Butane	58.124	272.7	4.14145	3192.9	2.86E-05	9.10E-05	257859.0	0.01154	-2.2E+07	83226.48
C_6	i-Pentene	70.135	303.1	4.99726	3154.9	2.86E-05	9.47E-05	232557.7	0.01242	-2.5E+07	84106.99
C_7	n-Pentane	72.150	309.2	5.14083	3146.4	2.86E-05	9.54E-05	228029.7	0.01259	-2.6E+07	84272.65
C_8	Pseudo-comp.	94.395	333.7	6.72578	2301.5	2.35E-05	1.41E-05	211453.3	0.00113	-2.8E+07	84906.36
C_9	Pseudo-comp.	112.199	378.6	7.99443	2391.1	2.44E-05	2.08E-05	186784.3	0.00466	-3.2E+07	85955.86
C_{10}	Pseudo-comp.	134.998	427.6	9.61887	2740.1	2.53E-05	2.84E-05	166503.7	0.00827	-3.7E+07	86967.39
C_{11}	Pseudo-comp.	159.573	472.5	11.36989	2700.7	2.60E-05	3.70E-05	152512.3	0.01120	-4.1E+07	87797.57
C_{12}	Pseudo-comp.	208.547	545.2	14.85938	2650.2	2.71E-05	6.05E-05	136703.0	0.01525	-4.9E+07	88988.10
C_{13}	Pseudo-comp.	315.751	659.3*	22.49784	2524.8	2.87E-05	1.50E-04	123745.0	0.02027	-6.0E+07	90568.21
C_{14}	Pseudo-comp.	436.709	749.3*	31.11639	2562.9	2.97E-05	3.24E-04	120705.6	0.02341	-7.0E+07	91631.33

* Estimated by area averaging of feed TBP curve

** Calculated assuming Ideal Gas Law

In the main program, solver options were specified to make pressure based calculations in a 3D space. Gradient calculation option was set to Green-Gauss cell based. Energy option, species transport model, specified reactions types, inlet diffusion, diffusion energy source, full multi-component diffusion and thermal diffusion were also enabled. On the materials and species forms, fifteen species, C_1 to C_{14} and C+ components were specified as pure component. All required physical properties of these components are listed in Table I. All properties of pure component (C_1 to C_7) were obtained from API Technical Data Book [15] except molecular weight, heat of vaporization, and entropy which were obtained from other sources. [14,16,17] On the other hand, properties of pseudo-component (C_8 to C_{14}) were calculated by using suitable methods given in API Technical Data Book [15] which are based on boiling point and specific gravity of each pseudo component. After problem definition, reaction kinetics was specified by manual entry of reaction name, reaction ID, reaction type, stoichiometric coefficients, Arrhenius rate pre–exponential factor, and activation energy for all 266 reactions in the 'Reactions' forms (Figure 2). Specification for the solid phase as "Catalyst" was made separately with solids density 1200 kg/m^3, and catalyst particle diameter 7.5x10^{-4}m. Methods for predicting other solid phase parameters such as granular viscosity, packing limits, etc., following models and options were selected.

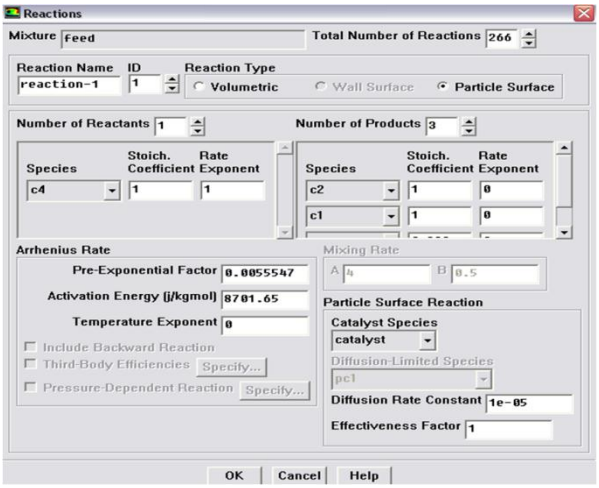

Fig. 2A Typical form to Feed in Reaction Kinetics Data for Cracking of C_4 Producing C_1 and C_2.

Granular Viscosity: Syamlal–Obrien model

Granular Bulk Viscosity: Lun et al. model

Frictional Viscosity: Schaeffer model

Solids Pressure: Syamlal–Obrien model

Radial Distribution: Syamlal–Obrien model

Angle of Internal Friction: 30 degrees

Packing Limit: 0.85

A constant value of 0.8 was taken for the coefficient of restitution. Catalyst and hydrocarbon feed were taken same as an actual industrial data [18]. The velocity and temperature of hydrocarbon feed was taken as 4.737m/s (20kg/s) and 496 K, respectively. Concentrations of all components other than C_{13} and C_{14} were specified zero as there is no cracking of hydrocarbons before entering riser. Catalyst was assumed to enter the riser at a temperature of 960K and velocity 0.295m/s (for C/O ratio of 7.2). Other parameters used in the simulator are listed in Table II.

RESULTS AND DISCUSSION

Industrial scale FCC plant data [18, 19, 23] (presented in Table II) were used in the present work. After initializing and feeding in all required information, simulation run was started on a personal computer. After attainment of convergence, results of the

Table II Parameters Used for the Simulation of Riser Reactor.

Parameter	*Value*	*Source*
C/O ratio	7.2	[18]
Catalyst particle density	1200 kg/m3	[19]
Catalyst temperature	960K	[18]
Specific heat of catalyst	1.15 kJ/kg K	[18]
Catalyst particle diameter	75 μm	[19]
Cluster diameter	6mm	[20]
Vol. fraction of clusters at inlet	0.5	[19]
Feed rate	20 kg/s	[18]
Feed temperature	496K	[18]
Specific gravity of feed	0.9292 g/cm3	[23]
Latent heat of feed vaporization	96 kJ/kg	[19]
Riser diameter	0.8m	[18]
Riser height	33m	[18]
Riser pressure	2.9 atm	[18]
Heat of combustion of coke	−32950 kJ/kg	[21]
Mass flow rate of steam	1.33 kg/s	[22]
Specific heat of steam	2.15 kJ/kg K	[22]

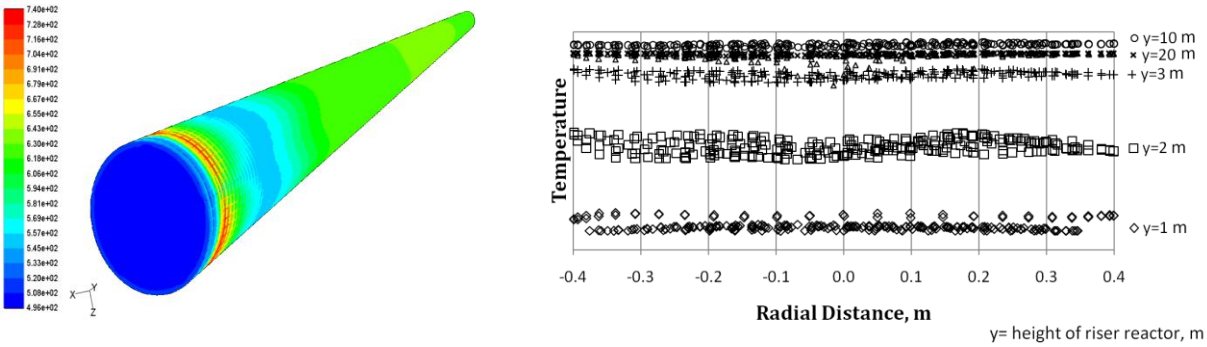

(a) 3D Contour (b) 2D Profile

Fig. 3 Vapor phase Temperature. (K)

riser reactor were analyzed. Three, dimensional and two dimensional vapor phase temperature profile are shown in Figure 3(a) and 3(b), respectively. Evidently, at the entrance vapor phase temperature (496 K) is equal to the specified feed temperature, however, it gain heat from catalyst and attains its maximum temperature (740 K) in 10 m from inlet and then decreases slightly due to endothermic cracking reaction. Here it should be noted that most of the theoretical investigators [2, 10, 24] reported increase of vapor phase temperature continues up to about 2 to 5 m only. This difference in prediction seems to be more realistic, as other model predicts cracking reaction completes within 20 m in place of 30 to 35 m of actual riser height [25]. This can be attributed to the fact that in the present simulation a realistic approach of turbulent flow condition is assumed. This is evident from continuously changing temperature and concentration in each volume element at a fixed location (Figure 3b). This indicate that an attempt to estimate average condition at a particular cross section of the riser, which is commonly done in other steady state models, would led to a larger degree of uncertainty.

Application of 3–dimentional fluctuating velocy model for FCC unit, revealed existence of "reaction bubble" in dense phase of fluidized bed, as shown in Figure 4. In this F`igure mass fractions of two

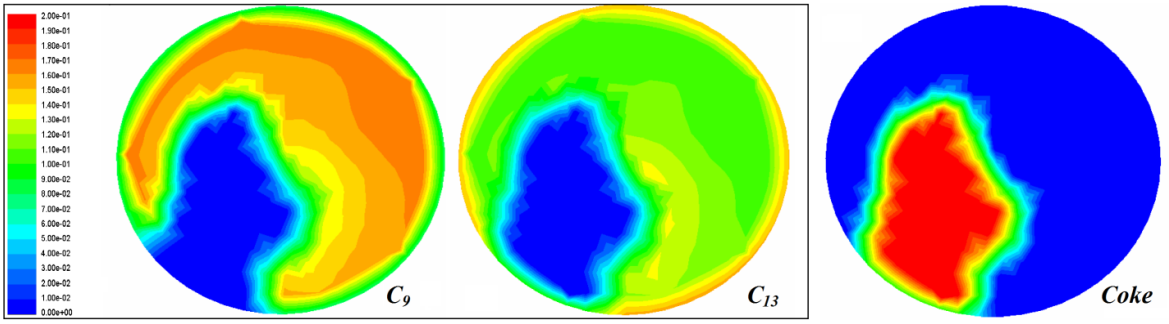

Fig. 4 Comparison of Mass Fractions at Exit of the Riser (Coke on Different Scale).

Pseudo–components (C_9 and C_{13}) along with coke at the riser exit are presented. At first sight it appears that a bubble (blue patch) in the the fluidized bed has formed that do not take part in reaction. In reality, however, this bubble like appearance is a region of low concentration of high molecular weight vapor components but contains high concentration of coke on catalyst. Interestingly, the catalyst concentration (not shown in the Figure) is almost uniform at this crosssection. Thus, high coke concentration indicate that in this region of fluidized bed, some time back, there was a vigorous cracking reaction through which all high molecular weight componds were cracked to produce component even lighter than C_9 leaving behind deactivated catalyst with a layer of coke deposites on it. Thus

formation of such over-reacting zones may be treated as "reaction buubles". A possible eplanation of nucleation sites required to initiate such intense reaction bubbles is avilable elsewhere [4]. According to this explanation one can expect that catalytic cracking is possible only at those places where concentrations of both catalyst and cracking species are high, e.g., bubble boundaries. Thus, it can easily be visualized that a favorable condition at the bubble boundary initiates cracking reaction which, almost instantaneously, deactivates the catalyst and reaction front moves deeper into the emulsion phase forming a reaction bubble.

Although, formation of vapor bubble is highly unexpected in a FCC riser, but some pockets (that moves up alongwith other materials) may form causing initiation of a "reaction bubble". This indicates that more rigorous investigation of FCC unit is required sothat the reactor operation can be optimized in a more efficient way. Perhaps this is why the overall yield predicted by many model such as Gupta et al., [2,10] (where continuous plug-flow condition is assumed), predicts that most of conversion take place within 20 m of reactor hight, whereas actual plant [25] requires more than 30m of riser height.

CONCLUSIONS

On the basis of results obtained in the present work, it can be concluded that under-prediction of riser height by various models [4] is mainly due to formation of "reaction bubbles". Proper accounting of this reaction bubble in FCC modeling is still a challenging task. Reaction kinetics available in open litrature are based on assumption of uniform reaction (or whole reactor volume), whereas due to formation of "reaction bubbles", only a fraction of total reaction volume is availabe. Therefore, a complete relook on the available rate constants of cracking reaction is required so that they can be used with more regorous three dimensional hydrodynamic models. Also, robust, computationally efficient hydrodynamic models are required to simulate turbulent three-phase flow.

REFERENCES

1. Gray J. H. and Handwerk G. E. *Petroleum Refining Technology and Economics*, 4/e, Marcel Dekker Inc., New York. 2001.
2. Gupta R. K. et al. *Chemical Engineering Science* 2007. 62. 4510–4528p.
3. FLUENT *Fluent 6.3 User Guide* Lebanon. 2005.
4. Kumar V. and Reddy A. S. K. *American Institute of Chemical Engineers Journal* doi: 10.1002/aic.12499. 2011, (Accepet).
5. Weekman V. W. Jr. *Industrial & Engineering Chemistry Process Design and Development* 1968. 7. 90–95p.
6. Weekman V. W. Jr. and Nace D. M. *American Institute of Chemical Engineers Journal* 1970. 16. 397–405p.

7. Lee L. et al. *Canadian Journal of Chemical Engineering* 1989. 67. 615–619p.
8. Corella J. et al. *Industrial & Engineering Chemistry Process Design and Development* 1991. 25. 554–562p.
9. Jacob S. M. et al. *American Institute of Chemical Engineers Journal* 1976. 22. 701–713p.
10. Benyahia. S. et al. *International Journal of Chemical Reactor Engineering* 2003. 1. A41.
11. Gupta R. K. and Kumar V. *Chemical Product and Process Modeling* 2008. 3. A11 http://www.bepress.com/cppm/vol3/iss1/11
12. Miquel J. and Castells F. *Hydrocarbon Processing* 1993. 72(12). 101–105p.
13. Miquel J. and Castells. F. *Hydrocarbon Processing*, 1994. 73(1). 99–103p.
14. Edmister W. C. and Lee B. I. *Applied Hydrocarbon Thermodynamics* Vol.2. Gulf Publishing Co., Houston, 1984.
15. API Technical Data Book. 1977.
16. Gopinathan N. and Saraf D. N. *Fluid Phase Equilibria* 2001. 179. 277–284p.
17. Luwei Zhao. et al. *Industrial and Engineering Chemical Research* 1999. 38. 324–327p.
18. Ali H. *Transactions of the Institution of Chemical Engineers*. 1997. 75. 410–412p.
19. Gupta A. and Subba Rao D. *Chemical Engineering Science* 2001. 56. 4489–4503p.
20. Fligner M. et al. *Chemical Engineering Science* 1994. 49. 5813–5818p.
21. Austin G. T. *Shreve's Chemical Process Industries* McGraw-Hill, Singapore. 1984.
22. Blasetti A. de Lasa. H. *Industrial and Engineering Chemical Research* 1997. 36. 3223–3229p.
23. Pekediz A. et al. *Industrial and Engineering Chemical Research* 1997. 36. 4516–4522p.
24. Souza J. A. et al. *American Institute of Chemical Engineers Journal* 2006. 52. 1895–1905p.
25. Derouin C. et al. *Industrial and Engineering Chemical Research* 1997. 36. 4504–4515p.